

# Light trapping in high-density ultracold atomic gases for quantum memory applications

I.M. Sokolov<sup>1,2</sup> and D.V. Kupriyanov<sup>1</sup>

<sup>1</sup>*Department of Theoretical Physics, State Polytechnic University, 195251, St.-Petersburg,*

<sup>2</sup>*Institute for Analytical Instrumentation, Russian Academy of Sciences, 198103, St.-Petersburg\**

R.G. Olave and M.D. Havey

*Department of Physics, Old Dominion University, Norfolk, VA 23529†*

(Dated: February 14, 2022)

High-density and ultracold atomic gases have emerged as promising media for storage of individual photons for quantum memory applications. In this paper we provide an overview of our theoretical and experimental efforts in this direction, with particular attention paid to manipulation of light storage (a) through complex recurrent optical scattering processes in very high density gases (b) by an external control field in a characteristic electromagnetically induced transparency configuration.

PACS numbers: 34.50.Rk, 34.80.Qb, 42.50.Ct, 03.67.Mn, 42.25.Dd, 42.50.-p

## I. INTRODUCTION

Manipulation of photonic degrees of freedom plays an important role in many aspects of quantum information sciences [1]. One of these is the storage of photonic information via a quantum memory, which forms an essential element of an optical quantum repeater [2]. One candidate for such a memory is an ultracold atomic gas [3], which can have such desirable qualities as very narrow and thus selectable resonance response, relative ease of manipulation of the atomic density, and precise control of many aspects of the atomic physical environment [4, 5]. Long lived atomic coherence may readily be generated, facilitating the formation, in lower density gases, of dark state polaritonic excitations using, for example, an optical  $\Lambda$  configuration [6–9]. Various environmental factors limit the lifetime of these coherences, and hence the time scale of efficient optical storage in the medium. An additional important factor that can limit the atomic coherence is multiple light scattering of near resonance radiation in an optically thick atomic ensemble [10]. Multiple light scattering in atomic gases is quasielastic, and so the scattered light can remain in a coherent state. This situation corresponds in the lower density case to the so-called weak localization regime, where such scattering can produce macroscopic observables such as the coherent backscattering cone [11–22]. The weak localization case is characterized by the inequality  $kl \gg 1$ , where  $k = 2\pi/\lambda$  is the light wave vector, and  $l$  is the mean-free path for light scattering. Such an effect promises to help clarify the role of multiple light scattering for quantum memory applications in this case. For much higher atomic densities, such that  $kl \sim 1$ , light scattering enters the so called strong localization regime. In

this case, recurrent light scattering can lead to formation of long lived atomic-photonic excitations which are currently under investigation as possible quantum memories, in searches for Anderson localization of light [23–27], development of atomic-physics based random lasers [28, 29], and for studies of single and multiple photon cooperative scattering [30, 31].

In this paper we provide a brief overview of our theoretical and experimental light storage programs using as approaches either light localization or electromagnetically induced transparency. This is accompanied by new results in several areas which illustrate some of the factors important in the physical processes. We concentrate particularly on the influence of multiple scattering in ultracold clouds, and its role in the timescale associated with quantum information storage.

## II. LIGHT STORAGE AND LIGHT LOCALIZATION

### A. Introduction

We have recently reported a comprehensive description of our theoretical approach to treatment of light scattering in very high density and ultracold atomic gases [32]. The atomic density used in these calculations corresponds closely to the Ioffe-Regel condition for light localization. In [32] we used two different but complementary approaches. In the first, we employed a self-consistent description of the atomic sample in the spirit of the Debye-Mie model for a macroscopic spherical scatterer consisting of a dense configuration of atomic dipoles. In the second, we take a microscopic approach in order to make exact numerical analysis of the quantum-posed description of the single photon scattering problem.

In the microscopic approach, the total scattering cross section can be determined by the T-matrix, which in turn can be expressed by the total Hamiltonian  $H = H_0 + V$  of

\*Electronic address: IMS@IS12093.spb.edu

†Electronic address: mhavey@odu.edu

the joint atomic-field system and by its interaction part  $V$  as  $T(E) = V + V(E - H)^{-1}V$ . In the rotating wave approximation the internal resolvent operator  $(E - H)^{-1}$  contributes to  $T(E)$  only by being projected on the states consisting of single atom excitation, distributed over the ensemble, and the vacuum state for all the field modes. Defining such a projector as  $P$  the projected resolvent  $\tilde{R}(E) = P(E - H)^{-1}P$  performs a finite matrix of size determined by the number of atoms  $N$  and the structure of the atomic levels. For the considered  $F = 0 \leftrightarrow F' = 1$  transition  $\tilde{R}(E)$  is a  $3N \times 3N$  matrix.

For a dipole-type interaction between atoms and field, the resolvent  $\tilde{R}(E)$  can be found as the inverse matrix of the following operator  $\tilde{R}^{-1}(E) = P(E - H_0 - VQ(E - H_0)^{-1}QV)P$ , where the complementary projector  $Q = 1 - P$ , operating in the self-energy term, can generate only two types of intermediate states: a single photon plus all the atoms in the ground state; and a single photon plus two different atoms in the excited state and others are in the ground level. For such particular projections there is the following important constraint on the interaction Hamiltonian:  $PVP = QVQ = 0$ , which is apparently valid for a dipole-type interaction  $V = -\sum \mathbf{d}_j \mathbf{E}_j$ , where  $\mathbf{d}_j$  is a dipole operator of the  $j$ -th atom and  $\mathbf{E}_j$  is the microscopic displacement field at the point where the atom is located. Due to this constraint the series for the inverse resolvent operator  $\tilde{R}^{-1}(E)$  is expressed by a finite number of terms and explicit analytical expression for  $\tilde{R}^{-1}(E)$  is obtained. The resolvent  $\tilde{R}(E)$  and T-matrix can be calculated numerically for an atomic system consisting of a several thousands of atoms. Thus, the microscopic approach gives us the exact value of the scattering amplitude for macroscopic atomic ensembles.

In this section, we present further elaboration of theoretical results obtained in [32], with particular emphasis on the spectral response of the total scattering cross section, and the time evolution of the total light scattered from a spherical and high density sample, because such evolution is strongly connected with light trapping in the cloud. We also present numerical results comparing the so-called vector and scalar approaches to the microscopic scattering problem. These important results show clearly that the frequently-used scalar model fails in a significant way for higher atomic densities  $\sim 5 \cdot 10^{13}$  atoms/cm<sup>3</sup>.

In this work, our theoretical discussion of time dependent scattering is based on the microscopic approach. The knowledge of the resolvent operator  $\tilde{R}(E)$  allows us to describe the interaction of the atomic ensemble with weak coherent light, which can be approximated as a superposition of the vacuum and single excitation states. Thus, considering the light pulse as a superposition of such coherent components, we generalize our approach to the case of non steady state.

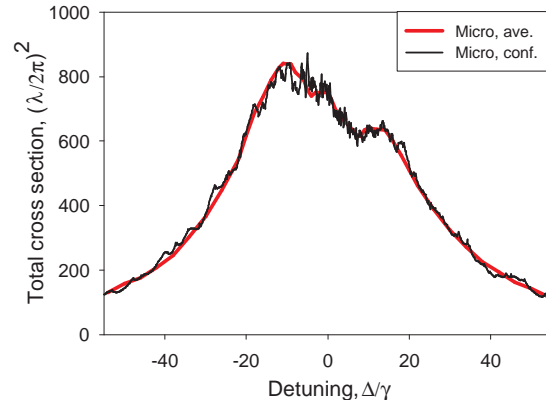


FIG. 1: The spectral dependence of the total cross sections for atomic samples of size  $10\lambda$  and density  $n_0\lambda^3 = 0.5$ . Calculations of the microscopic response for a particular configuration (black curve) indicates a micro-cavity structure generated by interatomic interactions in dense disordered media.

## B. Theoretical results

We first present in Fig. 1 the spectral variation of the total light scattering cross section from a dense spherical cloud of ultracold atoms. For these calculations the sample radius is  $10\lambda$  and the atom density  $n = n_0\lambda^3 = 0.5$ . As we mainly focus in our program on experiments with atomic Rb,  $\lambda = 780/2\pi$  nm, and the base unit of atomic density ( $n = 1$ ) corresponds to  $5.2 \cdot 10^{14}$  atoms/cm<sup>3</sup>. There are two results shown. The first corresponds to the scattering cross section for a single realization of the atomic sample. This means that there is a single configuration of atomic positions within the sample. The second result, indicated by the thicker curve (red on line), is the average result obtained from many such configurations of atomic positions. We first see that, in both cases, the spectral variations extend over a quite wide range, expressed in units of  $\gamma$ . This is qualitatively due to the high optical depth associated with transmission of light through the sample. Second, we observe that both the single realization and the configuration averaged cross sections contain broad oscillations which are primarily due to diffractive scattering from the nearly opaque spherical atomic sample. The most important feature of these results is the microstructure superimposed on the broad spectral variations. Of particular interest in the context of long lived photonic modes within the sample is the existence of the very narrow resonances apparent in the figure. These features arise from poles in the resolvent which have associated very narrow spectral widths. We point out that there is a nearly continuous spectral distribution of such poles, but that a significant fraction of them have associated narrow widths for higher atomic densities. In addition, we emphasize that the spectral locations of these poles are configura-

tion dependent; the resonance locations are different for different spatial arrangements of the atoms in the sample.

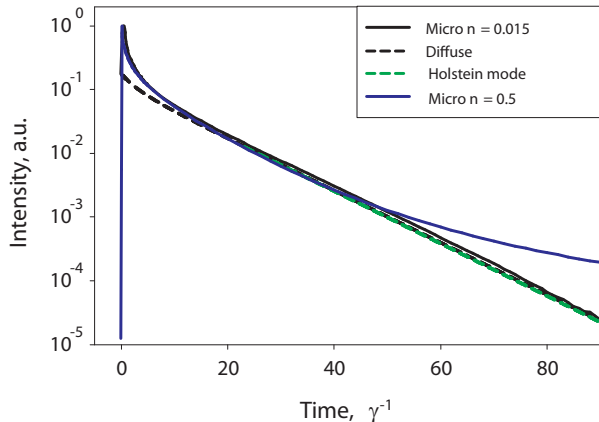


FIG. 2: Comparison of the time dependence of the scattered light intensity for spherical atomic clouds of different densities, but approximately constant optical depth. Preparation of the sample is made with a temporally short pulse having a correspondingly large enough bandwidth to cover the spectral response of the system, viz. Fig. 1. Microscopic results are compared with a diffusive model, and with the expected Holstein mode decay for each case.

The microstructure apparent in Fig. 1 implies that there will be long lived collective states present in any single configuration of the atomic sample. In the time domain, then, we can expect evolution of light scattered from the sample to have associated relatively slowly decaying components, measured in terms of the characteristic time scale  $1/\gamma$ . In Fig. 2 we show just such behavior for the conditions associated with the curves of Fig. 1. In the figure we first point out the characteristic exponential decay of the scattered light normally expected at lower densities. The three nearly identical curves correspond to a lower density microscopic calculation ( $n = 0.015$ ), to a solution to the diffusion equation for similar conditions, and to the decay constant corresponding to the longest lived Holstein mode. At the higher density associated with Fig. 1, we see a dramatic slowing of the decay of the intensity at the longest times. This slowing occurs in coincidence with the development of the spectral microstructure of Fig. 1, and corresponds to formation of subradiant atom-field collective modes in the sample.

The time evolution of the scattered light intensity also shows systematic variations with other experimentally accessible variables. For example, we show in Fig. 3 the longer time intensity decay for a spherical sample of radius  $10\lambda$  and several different atom densities. In Fig. 3 it is apparent that for higher densities the time scale for decay slows with increasing density, this being a reflection of the combined influence of the increasing diffusive decay time and the formation at higher densities of microresonances as in Fig. 1. We emphasize here that the time

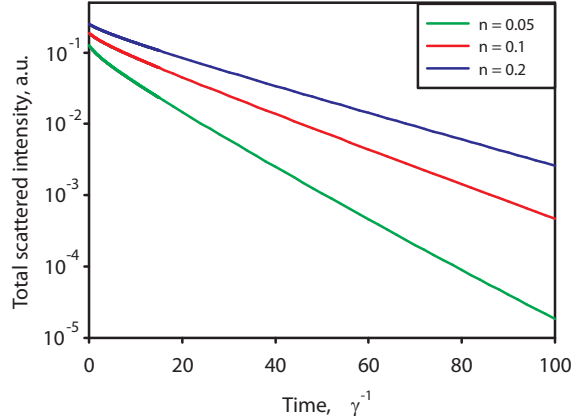


FIG. 3: Time dependence of the total scattered light intensity from a uniform spherical sample of atoms of radius  $10\lambda$  and several different atom densities. Preparation of the sample is made with a temporally short pulse having a correspondingly large enough bandwidth to cover the spectral response of the system, viz. Fig. 1.

evolution of the afterglow of the excited atomic sampled strongly depends on the conditions of excitation. For instance, the results in Fig. 2 and Fig. 3 are obtained for excitation of the cloud by a very short pulse, the spectrum of which encompasses the entire manifold of excited states of the ensemble. Alternatively, we can excite the cloud with a temporally longer pulse, one which has an associated narrower spectrum. This allows us to select spectral regions with the highest density of longer-lived states.

The long time exponential decay for two different spectral detunings from resonance are shown in Fig. 4. These curves correspond to excitation with a long, and thus spectrally narrow, pulse, as discussed in the previous paragraph. Shown are the associated decay constants, from which we see that the rate of decay is slower for larger detunings in this case. As discussed previously, this connects directly with the spectral distribution of collective states having different lifetimes; to be more precise, with the spectral distribution of resolvent poles with different imaginary parts. The existence of long lived states is determined by the strong interatomic interactions, which also causes large spectral shifts of such states. To effectively generate excitation of these states with a long pulse, we must use light with its central frequency essentially shifted from the free atom resonance frequency.

To close this section, we consider the results of Fig. 5. These calculations of the time evolution of the total light intensity are made for a spherical sample of density  $n = 0.1$  and show the clear effects of using a more-correct vector model of the light-matter microscopic interaction in comparison with a scalar one. Although we have shown such effects to be quite negligible for lower atomic den-

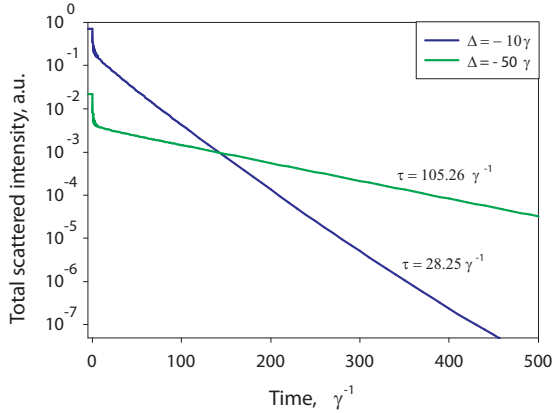


FIG. 4: Time dependence of the total scattered light intensity from a uniform spherical sample of atoms for two different detunings from bare resonance. Excitation is with a temporally long pulse, corresponding to a narrower pulse bandwidth than the results of Fig. 2-3. The atom density  $n = 0.1$ .

sities, for the higher density cases of importance to light trapping, light localization and random lasing, for example, the scalar approximation should not in general be made in order to obtain the most reliable results.

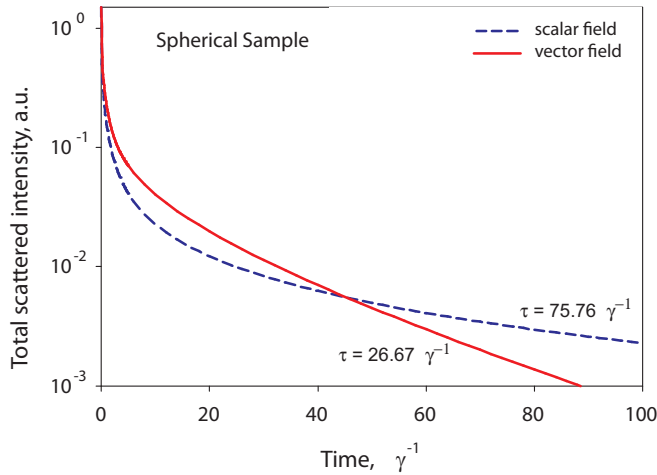


FIG. 5: Comparison of vector and scalar field results for the time evolution of the total scattered light intensity in a dense medium:  $n = 0.1$

### III. LIGHT STORAGE AND ELECTROMAGNETICALLY INDUCED TRANSPARENCY

#### A. Introduction

A second area of theoretical and experimental research interest in our group is multiple light scattering in a

medium dressed with a strong control field. In this section, we first present a synopsis of our theoretical approach and some results taken from Datsyuk, *et al.* [10]. This is followed by an overview of more recently completed initial experiments in a similar electronic  $\Lambda$  configuration [33]; these results indicate that, along with the forward scattered beam, the light scattered out of the coherent forward beam also propagates under conditions of electromagnetically induced transparency. Here we briefly summarize the theoretical and experimental approaches, but we refer the reader to those papers for detailed exposition of our theoretical and experimental studies, and focus here on some illustrative results.

#### B. Theoretical and experimental approaches and results

##### 1. Theory

Light transport in a dilute medium generally performs a diffusion-type process, which in a semiclassical picture can be visualized as a forwardly propagating wave randomly scattered by atoms in a sample. In an optically dense medium this process generates a zigzag-type path consisting of either macroscopically or mesoscopically scaled segments of forwardly propagating waves. To describe such a process theoretically we solve three problems. First we determine the scattering tensor amplitude for an arbitrary elementary incoherent scattering event. Then we describe forward propagation of the light between two successive incoherent scattering events. This is theoretically accomplished through the Green's function formalism. This function is completely described by the macroscopic susceptibility tensor of the atomic medium, which in the considered case of a cloud of ultracold atoms under EIT conditions is spatially inhomogeneous and optically anisotropic (for more detail, see [10]). In spite of this inhomogeneity and anisotropy we are able to solve analytically the system of Dyson-type equations for the polarization components of the retarded Green function for the light. Knowledge of the analytical expressions for both the scattering tensor and photon Green function allows us to solve the last, and third component of this problem, which is averaging over all possible random scattering chains. This is done through the framework of the procedure of Monte-Carlo simulation. Realization of this theoretical approach [10] allows us to describe the polarization, the spectral and the temporal properties of the scattered light.

One of the more important results from our earlier theoretical papers [10] is that the light scattered out of the coherent probe beam continues to propagate through multiple scattering in the medium dressed by the external control field. This means that the role of this light in the subsequent storage and retrieval of any photonic pulse has to be treated properly; that is, the coherence associated with the multiple scattering process has to be

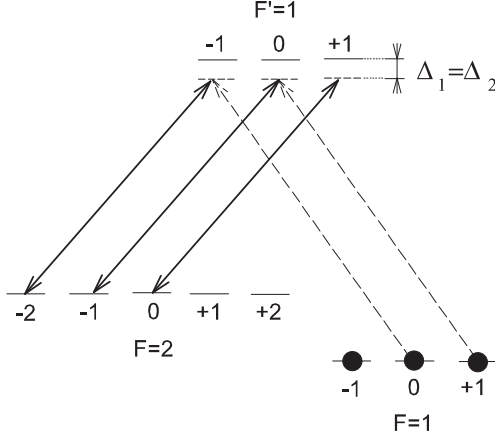


FIG. 6: An example of an excitation scheme for observation of the EIT effect in the system of hyperfine and Zeeman sub-levels of the  $D_1$ -line of  $^{87}\text{Rb}$ . The coupling field is applied with right-handed circular polarization to the  $F = 2 \rightarrow F' = 1$  transition and the probe mode in the orthogonal left-handed polarization excites the atoms on the  $F = 1 \rightarrow F' = 1$  transition. The EIT effect appears for equal detunings of the coupling and probe modes from atomic resonances:  $\Delta_1 = \Delta_2$

taken into account.

We have used the scheme of Fig. 6 to illustrate features of this effect. In that scheme, which refers to the  $D_1$ -line of  $^{87}\text{Rb}$ , the coupling field is applied with right-handed circular polarization to the  $F = 2 \rightarrow F' = 1$  transition. The probe mode, on the other hand, is applied in the orthogonal left-handed polarization and excites the atoms via the  $F = 1 \rightarrow F' = 1$  transition. The two fields are assumed to be in two-photon resonance. The temporal profile of the probe intensity is taken to be Gaussian with a width of  $100 \gamma^{-1}$ . The pulse reaches its peak intensity at a time  $t = 0$ . Examination of the results shown in Fig. 7 shows that the light emerging from the sample has a significant extension to longer times, particularly for the Rayleigh  $\sigma_+ \rightarrow h_-$  scattering channel. This is a manifestation of the well known slow-light effect in the scattering channels. This effect is normally associated with the forward scattering of the probe beam, but the results of [10] clearly show that the sample dressing by the control field plays a significant role in the scattered light dynamics. Finally, we point out that the temporal beating in the scattered light intensity is a result of the spectral distortion of the incident pulse by the EIT prepared medium. In other words, the Gaussian spectral distribution associated with the incident pulse is transformed by the medium, and particularly by the transparency associated with the EIT effect. The spectral hole generated in the probe spectrum results in beating at the frequency associated approximately with the width of the EIT transparency.

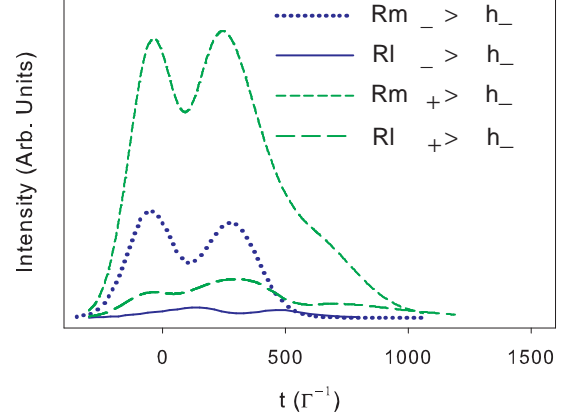


FIG. 7: The intensity profiles for the portion of the light pulse scattered at  $90^\circ$  to the direction of the incident pulse. The curves represent the Rayleigh (RI) channel ( $F = 1 \rightarrow F' = 1 \rightarrow F = 1$ ) and the Raman (Rm) channel ( $F = 1 \rightarrow F' = 1 \rightarrow F = 2$ ), with the input polarization state, and polarization channel of the emerging light as indicated in the caption. In all cases, the observation channel corresponds to detection of light with left-hand helicity ( $h_-$ ).

## 2. Experiment

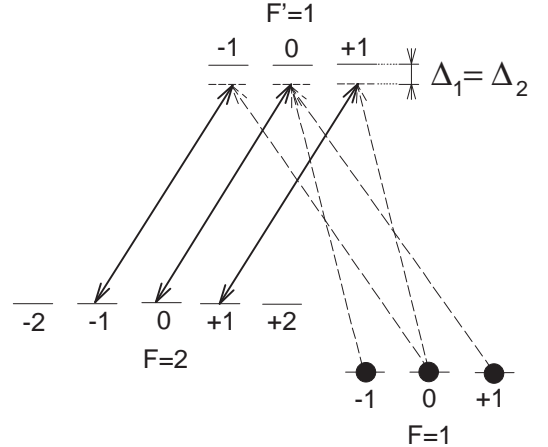


FIG. 8: Experimental probe and control field excitation configuration associated with the  $F = 1 \rightarrow F' = 1 \rightarrow F = 2$  transition of the  $D_2$  line in  $^{87}\text{Rb}$ . The control field is indicated by the solid lines, and the probe by dashed lines. The illustration corresponds to two photon resonance; Zeeman level light shifts  $\sim 1$  MHz associated with off resonance transitions are not shown.

The experimental program focuses on ultracold atomic samples prepared and confined in a magneto optical trap (MOT). We present here highlights of the experimental instrumentation: details are presented elsewhere [33]. The  $^{87}\text{Rb}$  MOT is arranged in a standard vapor loaded configuration, and consists of samples of about  $10^7$  atoms

with a Gaussian radius of 0.3 mm. The sample has an optical depth, on the  $F = 2 \rightarrow F' = 3$  trapping transition, of about 10, while the atom sample has a typical temperature  $\sim 100 \mu\text{K}$ . These samples are of sufficient optical depth that there can be several orders of multiple scattering of light scattered out of the probe beam. The excitation configuration we have used in our initial experiments to study the dynamics of the scattered light is shown in Fig. 8. In this scheme, the linearly polarized control field (z quantization axis) is tuned in the vicinity of the  $F = 2 \rightarrow F' = 1$  transition, while the much weaker linearly polarized (x direction) probe beam is tuned near the  $F = 1 \rightarrow F' = 1$  transition. The two lasers are characteristically tuned to be near two photon resonance, where  $\Delta_1 = \Delta_2$ . We point out that this configuration is not optimal for obtaining large orders of multiple scattering. The main reason for this is that there are open decay channels to the  $F = 2$ ,  $m = \pm 2$  states, in which population can be trapped for relatively long periods of time.

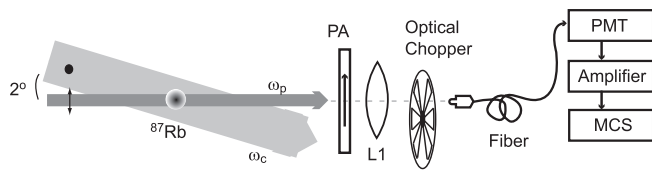


FIG. 9: Schematic diagram of the time evolution of transmitted, stored, and retrieved using the level scheme of Fig. 8. PA stands for polarization analyzer, PMT represents a photomultiplier tube, and MCS indicates a multichannel scalar.

The basic experimental approach is shown schematically in Fig. 9. In the figure, it is seen that the pump and control fields, depicted by  $\omega_p$  and  $\omega_c$ , respectively, propagate in approximately collinear fashion through the sample. The lasers are external cavity diode lasers, locked to saturated absorption resonances in a Rb vapor cell, and frequency tuned and switched in the conventional way with acousto optical modulators. Each laser has a long time average bandwidth on the order of 500 KHz. In these initial experiments, the two lasers are not mutually phase locked; the combined laser bandwidths then provide the ultimate limit to the characteristic ground state coherence lifetime. In the experiment, a small angle is arranged between them in order to suppress back-ground due to the much more intense control field on top of the relatively weak probe beam intensity. Further suppression is achieved by means of a linear polarization analyzer (PA) placed directly in the path of the probe and control beams. An optical chopper is used to minimize intense MOT fluorescence signals while the sample is being loaded; the chopper trigger is used as a master switch to initiate each data cycle, minimizing the relative absolute instability of the chopper timing. The probe laser beam is launched into an optical fiber which transmits the light to a photomultiplier operating in a photon counting mode. Following amplification of the individual

pulses, the signals are time sorted with up to 5 ns resolution in a multichannel scalar (MCS). The MCS also serves to accumulate and store the data for later analysis.

Under conditions of two photon resonance, and for typical control and probe field intensities, we have found that, in our experimental conditions, it takes about 500 ns for the transmitted light to reach an approximately steady state level. With this configuration, we have been able to observe slowed transmission of the forward scattered probe beam, and also to measure so-called stopped light pulses for a range of different delay times. In these measurements, which we present elsewhere [33], the control and probe fields are turned off in an approximately adiabatic way; later reapplication of the control field to the sample generates, from the dark state polariton, a retrieval of the forward scattered pulse. The lifetime of the regenerated pulses is quite short in the present experiment, and is limited by the mutual coherence of the ground state hyperfine levels. This in turn is determined by the relative phase instability of the control and probe fields. It is the storage and retrieval of such light pulses that provides an intriguing option for using EIT as the basis for an optical memory.

However, the primary focus of our projects is comparison of the forward scattered light with the sideways, or diffusely scattered light. To illustrate that comparison, we present in Fig. 10 the transparency in the forward scattered light as a function detuning of the weak probe beam from two photon resonance. These data were taken for a control field Rabi frequency of  $1.2 \gamma$ . From the figure, we see that there is a limited transparency in the transmitted light due to the relative sizes of the control Rabi frequency and the bandwidth due to the quite short ground state coherence time; larger control Rabi frequencies lead to nearly complete transparency [33]. The corresponding suppression of diffusely scattered light in the vicinity of two photon resonance is evident in the upper panel of Fig. 10. Theoretical analysis of the time evolution of this scattered light suggests that it propagates with a reduced group velocity, just as the forward scattered light. Our current projects are focused towards establishing the coherence properties of the multiply scattered light through observation of the coherent backscattering cone [10].

Finally, we point out that the present arrangement is not optimum, both because of the configuration used and because of the limited scale of the ground state coherence; further research is underway to extend this scale, and the amount of multiple scattering, in order to explore the role of coherent multiple scattering on the ultimate lifetime of light storage in ultracold and dense atomic gases. Further details of these experiments, including the effects of the control dressing field on the propagation of the light scattered from the probe pulse, are presented elsewhere [33].

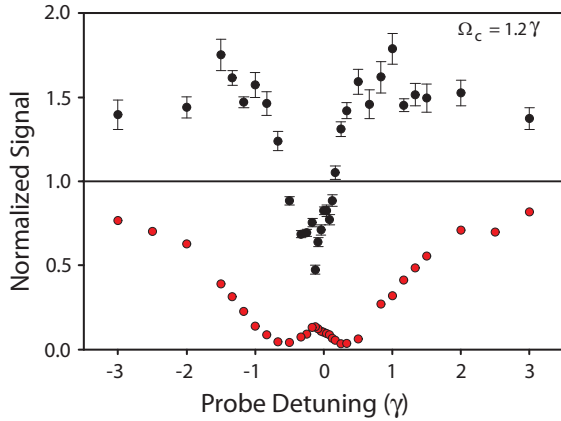


FIG. 10: Comparison of forward and diffusely scattered light using the level configuration of Fig. 8, and the experimental scheme of Fig. 9. The lower panel (red circles) refers to transmission, while the upper panel (black circles) refers to the diffusely scattered data. The data correspond variations of the weak probe laser frequency around two photon resonance, and to a control field Rabi frequency  $\Omega_c = 1.2 \gamma$ ; with reference to Fig. 8,  $\Omega_c$  refers to the average control Rabi frequency for the three indicated transitions.

#### IV. SUMMARY

In this paper we have briefly summarized some aspects of our theoretical and experimental studies of light stor-

age in dense and ultracold atomic gases. The two approaches we use have as a common theme the role of coherent multiple scattering in such media. For lower atomic densities, multiple scattering may serve as a limiting factor in photon storage time. There also is the intriguing possibility that a new type of quasiparticle, a diffuse dark state polariton, may be formed. Experiments in that direction are underway. For greater atomic densities, recurrent multiple scattering may lead to formation of long lived subradiant modes; these modes may serve in themselves as a means to store photonic information. Control of these modes may be achieved by manipulating dynamically the optical depth of the atomic media. One way to achieve this is through rapid control of the light shift of the involved atomic resonance levels.

#### V. ACKNOWLEDGMENTS

We appreciate the financial support of the Russian Foundation for Basic Research (Grant No. RFBR-08-02-91355), the National Science Foundation (Grant No. NSF-PHY-0654226).

- 
- [1] M.A. Nielsen and I.L. Chuang, *Quantum Computation and Quantum Information* (Cambridge University Press, 517 2000).
  - [2] H.-J. Briegel, W. Dur, J.I. Cirac and P. Zoller, Phys. Rev. Lett. 81, 5932 (1998).
  - [3] L.-M. Duan, M.D. Lukin, J.I. Cirac and P. Zoller, Nature 414, 413 (2001).
  - [4] Harold J. Metcalf and Peter van der Straten, *Laser Cooling and Trapping* (Springer-Verlag, New York, 1999).
  - [5] R. Grimm, M. Weidemuller, and Y. Ovchinnikov, Adv. At., Mol., Opt. Phys. 42, 95 (2000).
  - [6] M.D. Lukin, Rev. Mod. Phys. 75, 457 (2003).
  - [7] M.D. Lukin and A. Imamoglu, Nature 413, 273 (2001).
  - [8] T. Chaneliere, D.N. Matsukevich, S.D. Jenkins, S.-Y. Lan, T.A.B. Kennedy, and A. Kuzmich, Nature 438, 833 (2005).
  - [9] D. N. Matsukevich and A. Kuzmich, Science 306, 663 (2004).
  - [10] V.M. Datsyuk, I.M. Sokolov, D.V. Kupriyanov, and M.D. Havey, Phys. Rev. A 74, 043812 (2006); V. M. Datsyuk, I. M. Sokolov, D. V. Kupriyanov, and M. D. Havey Phys. Rev. A 77, 033823 (2008).
  - [11] Eric Akkermans and Gilles Montambaux, *Mesoscopic Physics of Electrons and Photons* (Cambridge University Press, Cambridge, UK, 2007).
  - [12] G. Labeyrie, F. de Thomasi, J.-C. Bernard, C.A. Muller, C. Miniatura, and R. Kaiser, Phys. Rev. Lett. 83, 5266 (1999).
  - [13] Y. Bidel, B. Klappauf, J.C. Bernard, D. Delande, G. Labeyrie, C. Miniatura, D. Wilkowski, and R. Kaiser, Phys. Rev. Lett. 88, 203902-1 (2002).
  - [14] D.V. Kupriyanov, I.M. Sokolov, N.V. Larionov, P. Kulatunga, C.I. Sukenik, and M.D. Havey, Phys. Rev. A 69, 033801 (2004).
  - [15] S. Balik, P. Kulatunga, C.I. Sukenik, M.D. Havey, D.V. Kupriyanov, and I.M. Sokolov, J. Mod. Optics 52, 2269 (2005).
  - [16] G. Labeyrie, C. Miniatura, and R. Kaiser, Phys. Rev. A 64, 033402 (2001).
  - [17] G. Labeyrie, C. Miniatura, C.A. Muller, O. Sigwarth, D. Delande, and R. Kaiser, Phys. Rev. Lett. 89, 163901-1 (2002).
  - [18] C.A. Müller, T. Jonckheere, C. Miniatura and D. Delande, Phys. Rev. A 64, 053804 (2001).
  - [19] D.V. Kupriyanov, I.M. Sokolov, and M.D. Havey, Optics Comm. 243, 165 (2004).
  - [20] M.D. Havey, Contemp. Phys. 50, 587 (2009).
  - [21] D.V. Kupriyanov, I.M. Sokolov, C.I. Sukenik, and M.D. Havey, Laser Phys. Lett. 3, 223 (2006).
  - [22] G. Labeyrie, Mod. Phys. Lett. B22, 73 (2008).
  - [23] P.W. Anderson, Phys. Rev. 109, 1492 (1958); P.W. Anderson, Philosophical Magazine 52, 505 (1985); E. Abra-

- hams, P.W. Anderson, D.C. Licciardello, and T.V. Ramakrishnan, Phys. Rev. Lett. 42, 673 (1979).
- [24] Ping Sheng, *Introduction to Wave Scattering, Localization, and Mesoscopic Phenomena* (Academic Press, San Diego, 1995).
  - [25] D. S. Wiersma, P. Bartolini, Ad Lagendijk, and R. Righini, Nature 390, 671 (1997).
  - [26] M. Storzer, P. Gross, C.M. Aegerter, and G. Maret, Phys. Rev. Lett. 96, 063904 (2006).
  - [27] M. Storzer, C.M. Aegerter, and G. Maret, Phys. Rev. E 73, 065602(R) (2006).
  - [28] W. Guerin, F. Michaud, and R. Kaiser, Phys. Rev. Lett. 101, 093002 (2008).
  - [29] L.S. Froufe-Perez, W. Guerin, R. Carminati, and R. Kaiser, Phys. Rev. Lett. 102, 173903 (2009).
  - [30] M.O. Scully, Phys. Rev. Lett. 102, 143601 (2009).
  - [31] A. A. Svidzinsky, J. Chang, and M.O. Scully, Phys. Rev. Lett. 100, 160504 (2008).
  - [32] D.V. Kupriyanov, I.M. Sokolov, M.D. Kupriyanova, and M.D. Havey, Phys. Rev. A 79, 053405 (2009).
  - [33] R.G. Olave, A.L. Win, M.D. Havey, I.M. Sokolov, and D.V. Kupriyanov, in preparation (2010).
  - [34] R. Zhang, S.R. Garner, and L.V. Hau, Phys. Rev. Lett. 103, 233602 (2009).
  - [35] R. Zhao, Y.O. Dudin, S.D. Jenkins, C.J. Campbell, D.N. Matsukevich, T.A.B. Kennedy, and A. Kuzmich, Nature Phys. 5, 100 (2009).
  - [36] L.V. Hau, S.E. Harris, Zachary Dutton, Cyrus H. Behroozi, Nature 397, 594 (1999).